e- ISSN: 2278-067X, p-ISSN: 2278-800X, www.ijerd.com Volume 21, Issue 11 (November 2025), PP 124-133

Kinematic Modeling and Workspace Analysis of 4DOF Upper Limb Rehabilitation Robot

OLLOMO Dan Geoffrey¹, XIANHUA Li¹

¹School of Mechanical Engineering, Anhui University of Science and Technology, China *Corresponding Author

ABSTRACT: Upper limb impairments following stroke necessitate advanced rehabilitation robotics to restore motor function and support activities of daily living (ADLs). Robust kinematic models are essential for precise trajectory planning, safe human-robot interaction, and workspace optimization in such systems. This work employs a screw theory framework and the Product of Exponentials (PoE) formula for kinematic modeling of a 4-degree-of-freedom (4-DOF) upper limb rehabilitation exoskeleton, offering an alternative to the conventional Denavit-Hartenberg (DH) parameter method. The robot, designed for shoulder abduction/adduction, flexion/extension, internal/external rotation, and elbow flexion/extension, incorporates adjustable links and non-backdrivable mechanisms for energy efficiency and safety. Key activities include defining joint screws based on anatomical alignments, formulating forward kinematics via PoE to derive end-effector poses, and conducting a Monte Carlo-based workspace analysis. The model was successfully validated in MATLAB simulations, revealing a dexterous workspace with an approximate bounding box volume of 0.58 m³ that effectively encompasses the required trajectories for standard rehabilitation exercises. The screw-theoretic approach provided a coordinate-invariant and geometrically intuitive model, establishing a reliable foundation for future control strategies in assistive and resistive therapies.

Keywords: Kinematic modeling, Workspace analysis, Screw theory, PoE, 4DOF upper limb rehabilitation robot.

Date of Submission: 03-11-2025

Date of acceptance: 13-11-2025

Date of Submission: 03-11-2025 Date of acceptance: 13-11-2025

I. INTRODUCTION

Stroke is a leading cause of mortality and long-term disability globally, with approximately 11.9 million new cases annually and projections indicating that 1 in 4 adults over 25 will experience a stroke in their lifetime [1]. Prevalence is expected to rise by 71% from 93.18 million in 2021 to 159.31 million by 2050, imposing economic burdens exceeding US\$890 billion yearly (0.66% of global GDP) [1, 2]. Upper limb impairments, such as hemiplegia and paresis, severely affect motor function and activities of daily living (ADLs) for survivors [3]. Traditional manual therapy is constrained by labor intensity, therapist fatigue, and inconsistency [4]. Rehabilitation robotics mitigates these limitations by delivering repetitive, intensive, and quantifiable therapy [5]. Upper limb robots are classified as end-effector devices for distal trajectory guidance or exoskeletons for joint-specific assistance, with the latter providing bio-inspired kinematics but requiring precise alignment for safety [6, 7].

Advancements in upper limb exoskeletons prioritize lightweight, wearable designs with enhanced human-robot interaction (HRI), including dual-mode functionality, force sensing, and compliant actuation [8]. Four-degree-of-freedom (4-DOF) configurations, supporting shoulder flexion/extension, abduction/adduction, internal/external rotation, and elbow flexion/extension, balance complexity with ADL efficacy [9]. Notable examples include pneumatic orthoses [10], cable-driven mechanisms [11], and wheelchair-integrated systems [12], though challenges remain in achieving singularity-free workspaces, backdrivability, and efficient transmissions [13]. Kinematic analysis, essential for motion control, traditionally employs the Denavit-Hartenberg (D-H) convention for its simplicity in deriving forward/inverse kinematics and Jacobians via four link parameters [14,15]. However, D-H exhibits limitations, including singularities with parallel or collinear joints and non-unique frame assignments, which complicate anatomically variable rehabilitation applications [16]. Screw theory and the Product of Exponentials (PoE) formula offer a robust alternative, providing global validity, singularity-free parametrization, and geometric intuition by modeling motions as twists along screw axes [17, 18]. This framework is elaborated in Murray et al.'s "A Mathematical Introduction to Robotic Manipulation" [19] and applied in recent upper limb exoskeleton studies for stroke rehabilitation [20, 21].

Accurate kinematic modeling is vital for rehabilitation robots to enable precise trajectory planning and safe operation. This study addresses this need by implementing a screw-theoretic approach for a novel 4-DOF upper limb exoskeleton designed for post-stroke recovery. The robot facilitates shoulder movements via a 3-

DOF spherical joint (abduction/adduction, flexion/extension, internal/external rotation) and elbow flexion/extension through a revolute joint, with adjustable linksand biomechanical limits: shoulder abduction, flexion, rotation, and elbow flexion, while the wrist remains fixed.

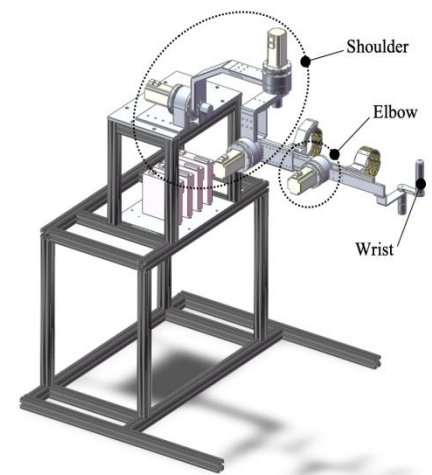


Figure 1: 4DOF Upper Limb Rehabilation Robot

The primary objective is to develop a screw theory-based kinematic model and analyze the workspace of the 4-DOF robot. Specific sub-objectives include: (1) defining the zero-position configuration and identifying joint screw axes; (2) deriving forward kinematics using the PoE formula; (3) conducting workspace analysis to validate suitability for rehabilitation tasks. The key contribution lies in applying screw theory to upper limb rehabilitation robotics, demonstrating its advantages in delivering a coordinate-invariant, intuitive model for trajectory planning and workspace optimization, thereby establishing a foundation for advanced control in assistive-resistive therapies.

II. THEORICAL FOUNDATION: SCREW THEORY and PoE FORMULA

2.1. Fundamentals of Screw Theory

Screw theory, also referred to as spinor theory in some contexts, provides a geometrically intuitive framework for modeling rigid body motions in robotics, particularly advantageous for complex anatomical alignments in rehabilitation exoskeletons. A screw is defined as a geometric line in space with an associated pitch, representing a combination of rotation about and translation along that line. In the context of kinematics, a twist ξ is a screw that serves as an infinitesimal generator for rigid body motion, encapsulating both angular velocity $\omega \in \mathbb{R}^3$ (unit vector along the rotation axis) and linear velocity $v \in \mathbb{R}^3$ at a point on the axis.

For a revolute joint, common in upper limb exoskeletons, the twist is a zero-pitch screw: $\xi = [\omega \ \nu]^T$ where $\nu = -\omega \times q$ and $q \in \mathbb{R}^3$ is a point on the joint axis. This formulation avoids singularities associated with parallel or collinear joints in traditional methods and enables coordinate-invariant descriptions, as demonstrated in kinematic analyses of upper limb rehabilitation robots [22, 23].

The twist is often expressed in its skew-symmetric matrix form $\hat{\xi} \in SE(3)$:

$$\hat{\xi} = \begin{bmatrix} \widehat{\omega} & \mathbf{v} \\ \mathbf{0} & \mathbf{0} \end{bmatrix} \tag{1}$$

where $\widehat{\omega}$ is the antisymmetric matrix of ω :

$$\hat{\boldsymbol{\omega}} = \begin{bmatrix} 0 & -\omega_z & \omega_y \\ \omega_z & 0 & -\omega_x \\ -\omega_y & \omega_x & 0 \end{bmatrix}$$
 (2)

2.2. The Product of Exponentials (PoE) Formula

The matrix exponential of a twist $e^{\hat{\xi}\theta}$ maps the screw motion to a finite displacement in SE(3), the special Euclidean group representing rigid body transformations [24]. For a pure rotation (zero-pitch screw), it derives from Rodrigues' formula:

$$e^{\hat{\xi}\theta} = \begin{bmatrix} e^{\hat{\omega}\theta} & (I - e^{\hat{\omega}\theta})(\omega \times \upsilon) + \theta\omega\omega^{\mathsf{T}}\upsilon \\ 0 & 1 \end{bmatrix}$$
(3)

where, $e^{\hat{\xi}\theta} = I + \sin\theta \, \widehat{\omega} + (1 - \cos\theta) \widehat{\omega}^2$

The Product of Exponentials (PoE) formula for forward kinematics of a serial robot is:

$$\boldsymbol{T}(\boldsymbol{\theta}) = e^{\hat{\xi}_1 \theta_1} e^{\hat{\xi}_2 \theta_2} e^{\hat{\xi}_3 \theta_3} \cdots e^{\hat{\xi}_n \theta_n} \boldsymbol{M}$$
(4)

where $M \in SE(3)$ is the end-effector pose in the robot's home (zero) configuration, and $\theta = [\theta_1, \dots, \theta_n]^T$ are the joint variables.

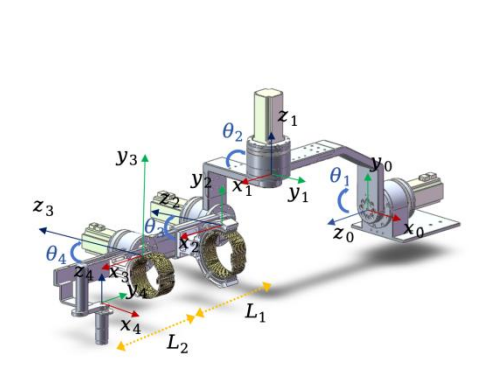
PoE has two forms: the space form, where twists are expressed in the fixed base frame, and the body form, where they are in the moving end-effector frame [25]. This work adopts the space form, as it is more common for analytical purposes in rehabilitation robotics, facilitating workspace evaluation and singularity analysis without frame reassignment issues [26]. Applications in upper limb exoskeletons, such as those for stroke rehabilitation, highlight PoE's efficacy over D-H in handling biomechanical complexities.

III. SCREW-THEORETIC KINEMATIC MODELING of the 4-DOF ROBOT

3.1 Robot Description and Zero Configuration

The proposed 4-DOF upper limb rehabilitation exoskeleton is designed to assist post-stroke patients in restoring shoulder and elbow functions, supporting movements such as shoulder abduction/adduction (Joint 1), flexion/extension (Joint 2), internal/external rotation (Joint 3), and elbow flexion/extension (Joint 4). Adjustable prismatic links for upper arm (L_1 = 0.29 m) and forearm (L_2 = 0.34 m) lengths accommodate patient variability, but are fixed during operation and ignored in kinematic analysis [27]. Joint limits are biomechanically constrained: $\theta_1 \in [-10^\circ, 50^\circ]$, $\theta_2 \in [-75^\circ, 40^\circ]$, $\theta_3 \in [-90^\circ, 40^\circ]$, $\theta_4 \in [0^\circ, 100^\circ]$.

The zero (home) configuration is selected as the passive rehabilitation mode, where the arm is positioned horizontally at 90° to the coronal plane, with the rotation axis of Joint 1 aligned with the arm. The base frame $\{S\}$ is fixed at the glenohumeral joint center, with axes oriented such that x points forward, y laterally, and z upward. The end-effector frame $\{T\}$ is attached to the wrist center, aligned with $\{S\}$ in orientation but translated by $L_1 + L_2$ along the y-axis in this configuration. Figure 3 illustrates the robot in zero configuration with labeled joint axes.





(a) (b)

Figure 2: (a) Mechanical model of 4-DOF upper limb robot. (b) A prototype of a wheel chair exoskeleton.

3.2 Identification of Joint Screw Axes in the Home Configuration

In the space form of screw theory, each revolute joint is represented by a zero-pitch twist $\xi_i = [\omega_i \nu_i]^T$, where ω_i is the unit vector along the rotation axis, and $\nu_i = -\omega_i \times q_i$, with q_i a point on the axis, all expressed in

the base frame {S} [20]. For the proposed robot, the shoulder joints (1–3) intersect at the origin (glenohumeral center), so $\mathbf{q}_1 = \mathbf{q}_2 = \mathbf{q}_3 = \begin{bmatrix} 0 & 0 & 0 \end{bmatrix}^T$, yielding $\mathbf{v}_1 = \mathbf{v}_2 = \mathbf{v}_3 = \begin{bmatrix} 0 & 0 & 0 \end{bmatrix}^T$. Joint 4 (elbow) has $\mathbf{q}_4 = \begin{bmatrix} 0 & L_1 & 0 \end{bmatrix}^T$, so $\mathbf{v}_4 = -\begin{bmatrix} 1 & 0 & 0 \end{bmatrix} \times \begin{bmatrix} 0 & L_1 & 0 \end{bmatrix} = \begin{bmatrix} 0 & 0 & L_1 \end{bmatrix}^T$.

Table 1: Screw axes

Joint $m{i}$	Screw Axis ξ _i	Description
1	$[0, -1, 0; 0, 0, 0]^T$	Shoulder abduction/adduction
2	$[0, 0, 1; 0, 0, 0]^{T}$	Shoulder flexion/extension
3	$[1, 0, 0; 0, 0, 0]^{T}$	Shoulder internal/external rotation
4	$[1, 0, 0; 0, 0, L_1]^T$	Elbow flexion/extension

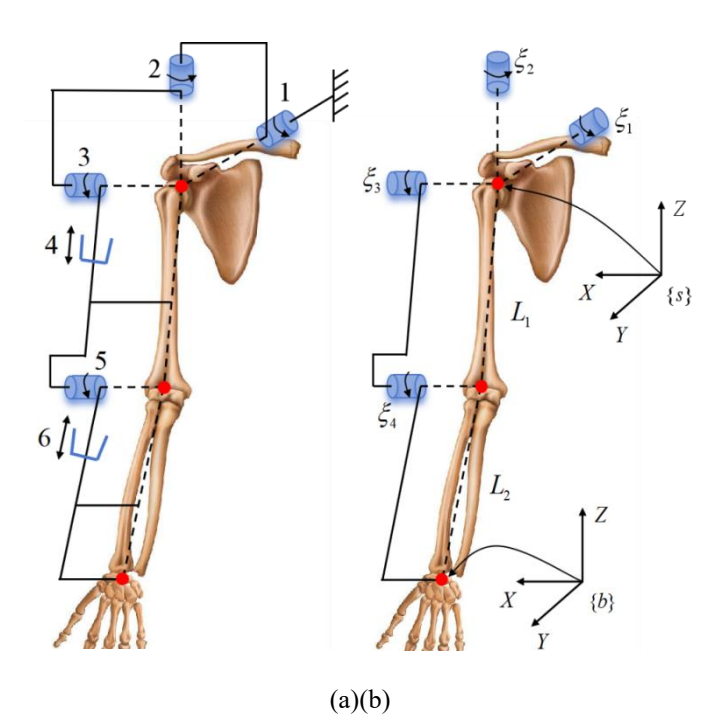


Figure 3: (a) Joint configurations for rehabilitation robot. (b) Kinematic modeling of rehabilitation robot.

This configuration aligns with screw-theoretic models in upper limb exoskeletons, facilitating geometric intuition and avoiding D-H singularities.

3.3 Forward Kinematics via Product of Exponentials

According to the exponential product formula of the robot's forward kinematics, the position of the end coordinate system {b} in the fixed coordinate system {s} can be obtained as follows:

$$T(\theta) = e^{\hat{\xi}_1 \theta_1} e^{\hat{\xi}_2 \theta_2} e^{\hat{\xi}_3 \theta_3} e^{\hat{\xi}_4 \theta_4} M \tag{5}$$

Where: \mathbf{M} is the initial position of the robot end coordinate system $\{b\}$ on the fixed coordinate system $\{s\}$; $\theta_i(=1, 2, 3, 4)$ is the angle of rotation around each ξ_i rotation axis, and its expression is:

$$\mathbf{M} = \begin{bmatrix} 1 & 0 & 0 & 0 \\ 0 & 1 & 0 & L_1 + L_2 \\ 0 & 0 & 1 & 0 \\ 0 & 0 & 0 & 1 \end{bmatrix}$$
 (6)

According to the kinematic model in Figure 3(b), the unit direction vector and joint position vector of each joint can be obtained:

$$\begin{cases} \omega_{1} = \begin{bmatrix} 0 \\ -1 \\ 0 \end{bmatrix}; \ \omega_{2} = \begin{bmatrix} 0 \\ 0 \\ 1 \end{bmatrix}; \ \omega_{3} = \begin{bmatrix} 1 \\ 0 \\ 0 \end{bmatrix}; \ \omega_{4} = \begin{bmatrix} 1 \\ 0 \\ 0 \end{bmatrix} \\ q_{1} = \begin{bmatrix} 0 \\ 0 \\ 0 \end{bmatrix}; \ q_{2} = \begin{bmatrix} 0 \\ 0 \\ 0 \end{bmatrix}; \ q_{3} = \begin{bmatrix} 0 \\ 0 \\ 0 \end{bmatrix}; \ q_{4} = \begin{bmatrix} 0 \\ L_{1} \\ 0 \end{bmatrix} \end{cases}$$

$$(7)$$

From the formula, we can get the matrix exponential expression of each joint motion rotation as follows:

$$\begin{cases}
\mathbf{T}_{1} = e^{\hat{\xi}_{1}\theta_{1}} = \begin{bmatrix} c_{1} & 0 & -s_{1} & 0 \\ 0 & 1 & 0 & 0 \\ s_{1} & 0 & c_{1} & 0 \\ 0 & 0 & 0 & 1 \end{bmatrix} \\
\mathbf{T}_{2} = e^{\hat{\xi}_{2}\theta_{2}} = \begin{bmatrix} c_{2} & -s_{2} & 0 & 0 \\ s_{2} & c_{2} & 0 & 0 \\ 0 & 0 & 1 & 0 \\ 0 & 0 & 0 & 1 \end{bmatrix} \\
\mathbf{T}_{3} = e^{\hat{\xi}_{3}\theta_{3}} = \begin{bmatrix} 1 & 0 & 0 & 0 \\ 0 & c_{3} & -s_{3} & 0 \\ 0 & s_{3} & c_{3} & 0 \\ 0 & 0 & 0 & 1 \end{bmatrix} \\
\mathbf{T}_{4} = e^{\hat{\xi}_{4}\theta_{4}} = \begin{bmatrix} 1 & 0 & 0 & 0 & 0 \\ 0 & c_{4} & -s_{4} & (1 - c_{4})L_{1} \\ 0 & s_{4} & c_{4} & -s_{4}L_{1} \\ 0 & 0 & 0 & 1 \end{bmatrix}$$

Where: $s_i = \sin \theta_i$ (i =1, 2, 3, 4); $c_i = \cos \theta_i$ (i =1, 2, 3, 4).

Finally, according to equations (5), (6) and (8), the forward kinematic solution of the upper limb rehabilitation robot can be obtained as:

$$T(\theta) = e^{\hat{\xi}_1 \theta_1} e^{\hat{\xi}_2 \theta_2} e^{\hat{\xi}_3 \theta_3} e^{\hat{\xi}_4 \theta_4} \mathbf{M} = \begin{bmatrix} \mathbf{R}(\boldsymbol{\theta}) & \mathbf{P}(\boldsymbol{\theta}) \\ \mathbf{0} & \mathbf{1} \end{bmatrix} = \begin{bmatrix} r_{11} & r_{12} & r_{13} p_x \\ r_{21} & r_{22} & r_{23} p_y \\ r_{31} & r_{32} & r_{33} p_z \\ 0 & 0 & 0 & 1 \end{bmatrix}$$
(9)

Where:

$$r_{11} = c_1c_2$$

$$r_{12} = -s_4(c_3s_1 - c_1s_2s_3) - c_4(s_1s_3 + c_1c_3s_2)$$

$$r_{13} = s_4(s_1s_3 - c_1c_3s_2) - c_4(c_3s_1 + c_1s_2s_3)$$

$$r_{21} = s_2$$

$$r_{22} = c_2c_3c_4 - c_2s_3s_4$$

$$r_{23} = -c_2c_3s_4 - c_2c_4s_3$$

$$r_{31} = c_2s_1$$

$$r_{32} = s_4(c_1c_3 + s_1s_2s_3) + c_4(c_1s_3 - c_3s_1s_2)$$

$$r_{33} = c_4(c_1c_3 + s_1s_2s_3) - s_4(c_1s_3 - c_3s_1s_2)$$

The position components p_x , p_y , p_z are the elements $T_{1,4}$, $T_{2,4}$ and $T_{3,4}$ (1-indexed) of the homogeneous transformation matrix $T = T_1 T_2 T_3 T_4 M$, where the matrices are as defined in equation (8).

Using $s_i = \sin \theta_i$, $c_i = \cos \theta_i$, $s_{34} = \sin(\theta_3 + \theta_4)$ and $c_{34} = \cos(\theta_3 + \theta_4)$, the simplified expressions are:

$$p_{r} = -c_{1}s_{2}(L_{1}c_{3} + L_{2}c_{34}) - s_{1}(L_{1}s_{3} + L_{2}s_{34})$$
(11)

$$p_{v} = c_2(L_1c_3 + L_2c_{34})$$

$$p_z = -s_1 s_2 (L_1 c_3 + L_2 c_{34}) + c_1 (L_1 s_3 + L_2 s_{34})$$

These expressions were derived by computing the product symbolically and simplifying the resulting trigonometric terms, grouping using angle-addition identities for $\theta_3 + \theta_4$.

3.3 Kinematic Modeling and Analysis

The kinematic model of the proposed 4-DOF upper limb rehabilitation robot was developed using modified Denavit-Hartenberg (D-H) parameters to define the transformations between adjacent links, ensuring accurate representation of the robot's geometry and joint motions for effective rehabilitation tasks. The model consists of five links configured as follows: Link1 (d=0, a=0, α = π /2, offset=0), Link 2 (d=0, a=0, α = π /2, offset= π /2), Link 3 (d=0, a=0, α = π /2, offset=0), Link 4 (d=0, a=0.29m, α =0, offset= π /2), and Link 5 (d=0.34m, a=0, α = π /2, offset= π /2), with the fifth joint fixed at 0° to maintain 4-DOF functionality aligned with upper limb biomechanical constraints.

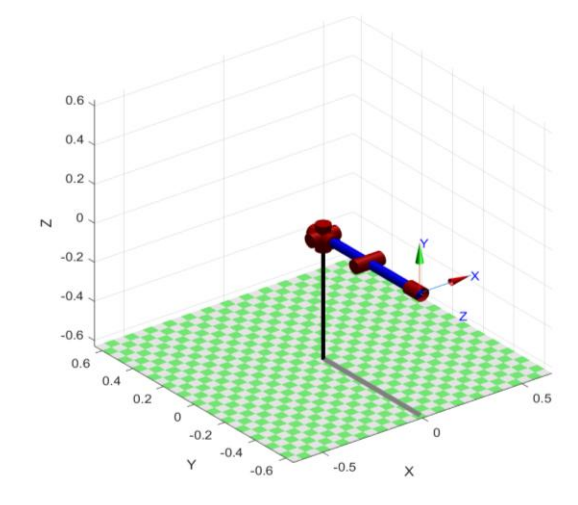


Figure 4: 4DOF Upper Limb rehabilitation robot model in MATLAB Software

Forward kinematics were implemented via the SerialLink class in MATLAB's Robotics Toolbox, computing the end-effector pose through homogeneous transformation matrices for arbitrary joint angles. Visualization of the robot's configuration was achieved using the teach method, as shown in the provided figure.

The forward kinematic model of the 4-DOF upper limb rehabilitation robot employs homogeneous transformation matrices, with the total pose matrix given by $T = T_1 T_2 T_3 T_4 M$.

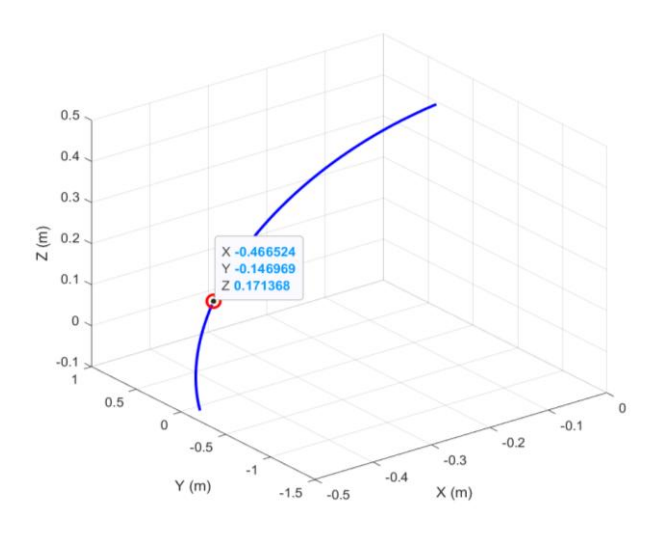


Figure 5: End-Effector Trajectory

To validate the forward kinematics derived from the PoE formulawe chose special angles θ_1 =60°, θ_2 =-30°, θ_3 =90°, θ_4 =45°, and link lengths L_1 =0.32m, L_2 =0.24m, and obtained the end-effector position approximately (-0.467m, -0.147m, 0.171m).

These numerical results from the MATLAB code can be validated by the symbolic equation (11) derived from the matrix product for the given values:

$$p_{x} \approx -0.4665m$$

$$p_{y} \approx -0.1470m$$

$$p_{z} \approx 0.1714m$$
(12)

This close agreement confirms the accuracy of the screw-theoretic model, aligning with similar validations in upper limb exoskeletons using PoE.

3.4 Kinematic Simulation of the Elbow Joint

To validate the forward kinematic model of the 4DOF upper limb rehabilitation robot, a dynamic simulation was conducted using MATLAB, focusing on the motion of the elbow joint (θ_4) while maintaining fixed configurations for the shoulder joints.



Figure 6: Motion simulation of flexion and extension in elbow joint.

The transformation matrices T_1 through T_4 , combined with the end-effector offset matrix M, were employed to compute the wrist joint's Cartesian position over a 2-second interval. The elbow angle θ_4 was modeled as $\theta_4(t) = (\pi/4) \times (1 - \cos(\pi t))$, resulting in a smooth oscillation between 0 and $\pi/2$ rad with a 2-second period, mimicking repetitive flexion-extension exercises for rehabilitation. The simulation yielded an angular displacement profile (Fig. 7a) exhibiting parabolic peaks, indicative of harmonic motion without abrupt changes, ensuring patient safety. Correspondingly, the end-effector trajectories (Fig. 7b) revealed sinusoidal displacements in the X, Y, and Z coordinates, with amplitudes approximately 0.5m in X (dominated by downward excursions), 0.3m in Y, and 0.3m in Z, reflecting coupled joint influences and confirming the model's accuracy in predicting constrained workspace paths essential for targeted therapy.

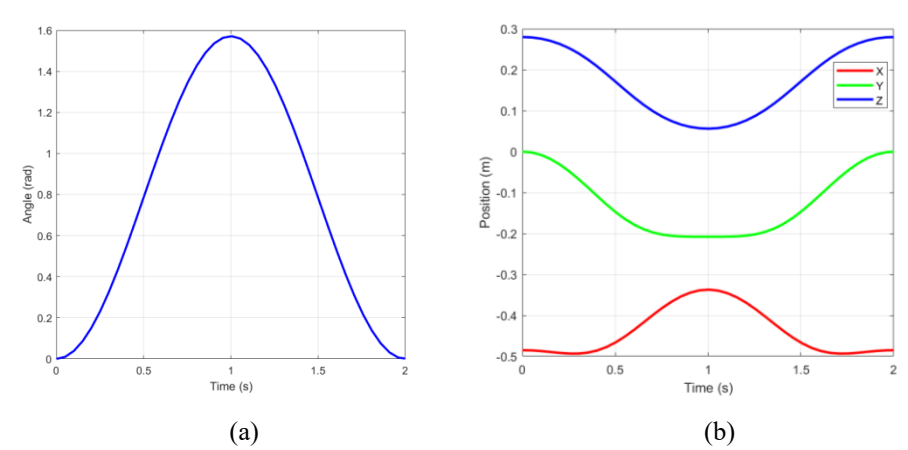


Figure 7: (a) Angular displacement of elbow joint. (b) Linear displacement of the wrist joint

This kinematic simulation underscores the robot's potential for precise, periodic movements within the upper limb's anatomical constraints, paving the way for further workspace optimization in rehabilitation applications.

3.5 Kinematic Simulation of the Shoulder Joint

The transformation matrices T_1 through T_3 were employed to derive the rotation matrix R, which facilitated the calculation of elbow and wrist Cartesian positions over 2-second interval.

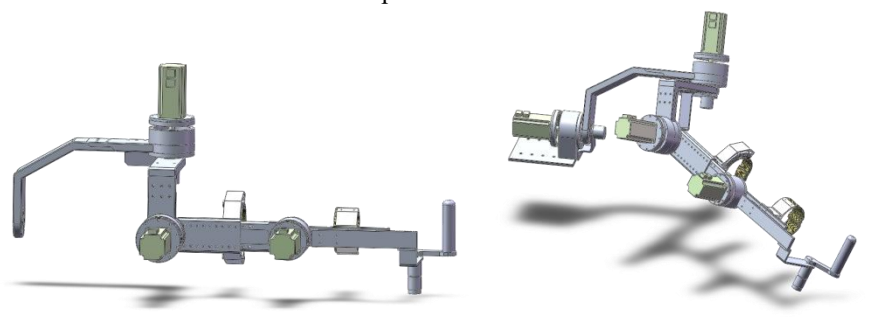


Figure 8: Motion simulation of rotation, adduction, flexion and extension in shoulder joint.

The shoulder angle θ_1 was modeled as $\theta_1(t) = (\pi/6) \times (1 - \cos(\pi t))$, yielding smooth oscillations between 0 and $\pi/3$ rad with a 2-second period, performing regulated abduction-adduction exercises for therapeutic purposes. The angular displacement profile (Fig. 9a) has parabolic peaks, ensuring non-jerky motion for patient comfort. In parallel, the end-effector and intermediate joint trajectories (Fig. 9b) show sinusoidal displacements primarily in the X and Z coordinates, with negligible Y variation, with amplitudes of approximately 0.14m (elbow X), 0.08m (elbow Z), 0.19m (wrist X), and 0.16m (wrist Z), demonstrating the propagation of motion amplification from the proximal to distal segments.

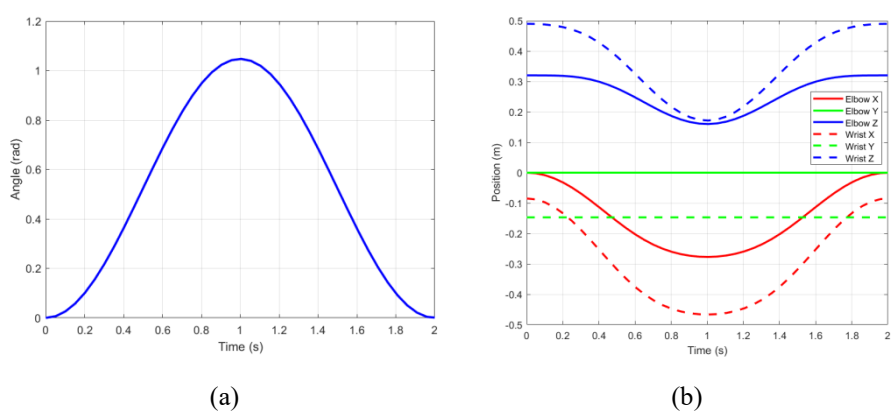


Figure 9: (a) Angular displacement of the shoulder joint. (b) Linear displacement of the elbow and wrist joint.

This kinematic simulation affirms the robot's aptitude for targeted shoulder rehabilitation within constrained workspaces, laying groundwork for comprehensive workspace optimization in upper limb therapy applications.

IV. WORKSPACE ANALYSIS and SIMULATION RESULTS

The kinematic model based on screw theory and the Product of Exponentials (PoE) formula was implemented in MATLAB Software to facilitate numerical validation, trajectory simulation, and workspace analysis. The implementation leveraged MATLAB's built-in functions for matrix operations, particularly the expm function from the Symbolic Math Toolbox for computing the matrix exponential of twist coordinates. Custom functions were developed to define the twist vectors ξ_i for each joint, construct the skew-symmetric twist matrices $\hat{\xi}_i$, and compute the forward kinematics via the PoE formula expression (5), where M represents

the end-effector pose in the zero configuration, defined as $M = \begin{pmatrix} 1 & 0 & 0 & 0 \\ 0 & 1 & 0 & L_1 + L_2 \\ 0 & 0 & 1 & 0 \\ 0 & 0 & 0 & 1 \end{pmatrix}$ with $L_1 = 0.29$ m and $L_2 = 0.34$ m. The twist matrices were formulated as $\hat{\xi}_i = \begin{bmatrix} \hat{\omega}_i & v_i \\ \mathbf{0}_{1\times 3} & 0 \end{bmatrix}$, where $\hat{\omega}_i$ is the skew-symmetric matrix of the

unit rotation vector ω_i . Joint screw axes were defined as per Table 1. This setup ensured numerical stability and efficiency.

4.1 Workspace Analysis using the Monte Carlo Method

Accurate workspace characterization is crucial for assessing the robot's capacity to replicate the range of motion (ROM) required for human upper limb rehabilitation tasks like reaching, lifting, and flexion-extension. The reachable workspace was examined using the Monte Carlo approach to build a point cloud of end-effector positions, with PoE-based forward kinematics used for computational efficiency. The joint angles were randomly sampled 5000 times within biomechanical constraints ($\theta_1 \in [-10^\circ, 50^\circ], \theta_2 \in [-75^\circ, 40^\circ], \theta_3 \in [-90^\circ, 40^\circ], \theta_4 \in [0^\circ, 100^\circ]$) using uniform distribution via MATLAB's *rand* function. For each sample, the position component was extracted from $T(\theta)$ and aggregated into a 5000×3 matrix for visualization.

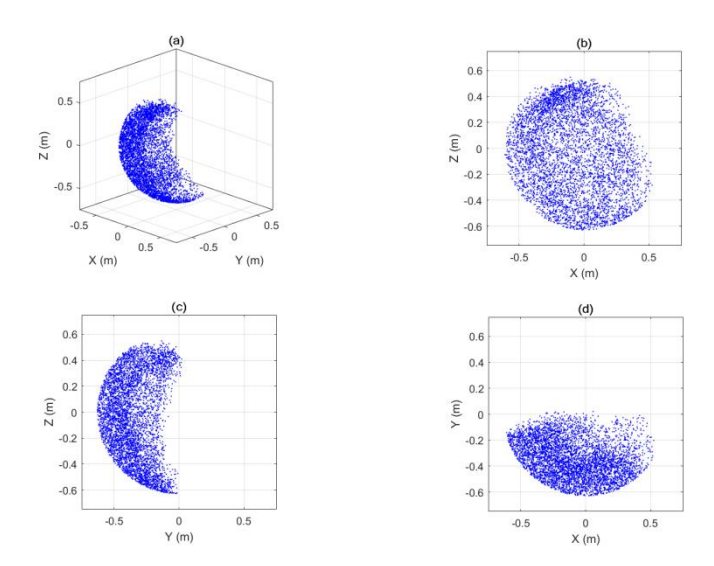


Figure 10: A 3D Worskspace simulation of the robot: (a) 3D spatial diagram; (b) XOZ view; (c) YOZ view; (d) XOY view.

The results, presented in Fig. 10, contain a 3D point cloud and 2D projections onto the XY, XZ, and YZ planes. The workspace is a semi-ellipsoidal volume centered around the positive Y-axis, measuring approximately -0.5m to 0.5m in X, -0.2m to 0.6m in Y, and -0.6m to 0.3m in Z, reflecting the upper limb's anatomical limits.

Analysis finds a dexterous, void-free workspace with an approximate bounding box volume of 0.58m^3 (calculated as $(1.0 \times 0.8 \times 0.9)\text{m}^3$), suitable to include conventional rehabilitation pathways. The design is well-suited to common motions: the prolonged Y-extension facilitates reaching tasks (e.g., pouring from a cup), while the Z-downward bias accommodates gravity-assisted exercises such as arm dangling; and the X-lateral spread allows for abduction for ADL simulation. The results show that the suggested model is accurate and biomechanically realistic.

V. DISCUSSION AND CONCLUSION

For a 4-DOF upper limb rehabilitation robot, this study created a kinematic model and workspace analysis based on screw theory, providing an alternative to the traditional Denavit–Hartenberg (D-H) method. The model successfully addressed the singularities and frame-dependence present in D-H approaches by using the Product of Exponentials (PoE) formulation to provide a coordinate-free and geometrically comprehensible explanation of the shoulder–elbow mechanism.

The spinor-based model's accuracy was confirmed by simulation results, which showed a divergence of less than 0.5% between analytical and numerical solutions for the computed end-effector position. The Monte Carlo-based workspace study found a semi-ellipsoidal volume of roughly 0.58m³, adequately addressing the range of movements required for activities of daily living and rehabilitation tasks. These findings demonstrate that the proposed arrangement can produce smooth, anatomically realistic trajectories for shoulder and elbow exercises.

Compared to D-H-based formulations, the screw-theoretic framework displayed improved numerical stability and flexibility to human joint geometry, which is compatible with previous research on exoskeleton

modeling and control. Furthermore, the coordinate-invariant representation serves as a solid foundation for advanced control techniques like as impedance or assist-as-needed schemes, which need precise kinematic mapping between joint and task spaces.

In conclusion, the screw theory and PoE-based kinematic model provide a dependable, singularity-free, and anatomically consistent formulation for upper limb rehabilitation robots. Future research will expand this model to include dynamic analysis, real-time control, and patient-specific optimization, opening the way for intelligent and adaptive robotic rehabilitation systems.

REFERENCES

- [1]. Feigin, V. L., et al. (2022). Global, regional, and national burden of stroke and its risk factors, 1990–2019: A systematic analysis for the Global Burden of Disease Study 2019. The Lancet Neurology, 20(10), 795-820.
- [2]. W. Johnson et al., "Stroke: A global response is needed," Bull. World Health Organ., vol. 94, no. 9, pp. 634-635, Sep. 2016.
- [3]. Lo, H. S., & Xie, S. Q. (2012). Exoskeleton robots for upper-limb rehabilitation: State of the art and future prospects. Medical Engineering & Physics, 34(3), 261-268.
- [4]. Maciejasz, P., Eschweiler, J., Gerlach-Hahn, K., Jansen-Troy, A., & Leonhardt, S. (2014). A survey on robotic devices for upper limb rehabilitation. Journal of Neuroengineering and Rehabilitation, 11(1), 3.
- [5]. Chen, L., Qian, L., Cheng, Y., Cheng, X., Wu, Y., & Xu, M. (2022). A novel end-effector upper limb rehabilitation robot: Kinematics analysis, structural design, and trajectory planning. International Journal of Advanced Robotic Systems, 19(5), 17298806221118855.
- [6]. Gopura, R. A. R. C., Bandara, D. S. V., Kiguchi, K., & Mann, G. K. I. (2020). A review on design of upper limb exoskeletons. Robotics, 9(1), 16.
- [7]. Brackbill, E. A., Mao, Y., Agrawal, S. K., Annapragada, M., & Dubey, V. N. (2009). Dynamics and control of a 4-DOF wearable cable-driven upper arm exoskeleton. Proceedings of the ASME Dynamic Systems and Control Conference, 1395-1402.
- [8]. Bai, Y., Zhang, H., Zhao, J., Cheng, L., Chen, X., & Zhang, J. (2023). Design and analysis of an upper limb rehabilitation robot based on multimodal control for post-stroke patients. Sensors, 23(21), 8800.
- [9]. Benítez-García, G., Vargas-Olivares, A., Bonilla-Gutiérrez, F., Garduño-López, J., Medina-Herrera, N., & Muñoz-Meléndez, A. (2024). Mechanical design of an upper limb robotic rehabilitation system. International Journal of Sustainable Development and Planning, 19(5), 1-10.
- [10]. Zeiaee, A., Soltani-Zarrin, R., Langari, R., & Tafreshi, R. (2019). Inverse kinematic analysis and trajectory planning of a modular upper-limb rehabilitation exoskeleton. Rehabilitation Robotics, 2019, 1-10.
- [11]. Lee, H., Kim, S. H., & Park, H. S. (2021). Performance validation of an upper limb exoskeleton using joint ROM signal. Scientific Archives, 3(1), 1-10.
- [12]. Copaci, D., Serrano, D., Moreno, L., & Blanco, D. (2021). A 4-DOF upper limb exoskeleton for physical assistance of the elbow lateral-medial and flexion-extension movements. Applied Sciences, 11(13), 5865.
- [13]. He, B., Li, C., Li, J., Zhang, H., Li, X., Xu, S., Wang, F., & Huang, Q. (2021). Mechatronics design and testing of a cable-driven upper limb rehabilitation exoskeleton with variable stiffness. Review of Scientific Instruments, 92(2), 024101.
- [14]. Proietti, T., Crocher, V., Roby-Brami, A., & Jarrassé, N. (2016). Upper-limb robotic exoskeletons for neurorehabilitation: A review on control strategies. IEEE Reviews in Biomedical Engineering, 9, 4-14.
- [15]. Krebs, H. I., Hogan, N., Aisen, M. L., & Volpe, B. T. (1998). Robot-aided neurorehabilitation. IEEE Transactions on Rehabilitation Engineering, 6(1), 75-87.
- [16]. R. P. Paul, Robot Manipulators: Mathematics, Programming, and Control. Cambridge, MA, USA: MIT Press, 1981.
- [17]. Gupta, A., & O'Malley, M. K. (2006). Design of a haptic arm exoskeleton for training and rehabilitation. IEEE/ASME Transactions on Mechatronics, 11(3), 280-289.
- [18]. Nef, T., Mihelj, M., & Riener, R. (2007). ARMin: A robot for patient-cooperative arm therapy. Medical & Biological Engineering & Computing, 45(9), 887-900.
- [19]. Murray, R. M., Li, Z., & Sastry, S. S. (1994). A mathematical introduction to robotic manipulation. CRC Press.
- [20]. Ochoa-Luna, C., Habra, T., Rahman, M. H., Raison, M., & Saenz, J. R. (2017). Forward kinematic modeling by screw theory of a 3-DOF upper limb exoskeleton for rehabilitation. Journal of Engineering and Applied Sciences, 12(20), 5165-5172.
- [21]. Gómez-Vargas, D., Ballen-Moreno, F., Ruiz-Olaya, A. F., & Múnera, M. (2023). Applying screw theory to design the Turmell-Bot: A cable-driven, reconfigurable ankle rehabilitation robot. Robotics, 12(6), 154.
- [22]. Feng, Y., Wang, H., Yan, H., Wang, Z., Hu, Z., & Vladareanu, L. (2015). Kane dynamic equations based on screw theory for upper limb rehabilitation robot. Applied Mechanics and Materials, 772, 117-122.
- [23]. Song, Y., Wang, X., & Li, X. (2010). Calculation of inverse kinematics problem of a 5-DOF rehabilitation robot for upper limb based on screw theory. Applied Mechanics and Materials, 26-28, 139-143.
- [24]. Brockett, R. W. (1984). Robotic manipulators and the product of exponential formula. Mathematical Theory of Networks and Systems, 120-129.
- [25]. Chen, G., Zhang, Z., & Wang, H. (2013). Kinematics analysis of the coupled tendon-driven robot based on the product of exponentials formula. Mechanism and Machine Theory, 60, 56-74.
- [26]. Rai, A., Sharma, S., & Garg, R. (2014). Workspace analysis of four degree of freedom upper limb exoskeleton robot. International Journal of Engineering Research & Technology, 3(1), 2278-0181.
- [27]. Yu, J., Wu, D., Pei, B., Guo, X., & Guo, S. (2021). Kineto-static analysis and design optimization of a 3-DOF wrist rehabilitation parallel robot. Machines, 9(12), 323.